*Laser and Particle Beams* (2006), *24*, 437–445. Printed in the USA.

DOI: 10.1017/S0263034606060381

# Improved equation of state of metals in the liquid-vapor region

A. RAY, M.K. SRIVASTAVA, G. KONDAYYA, AND S.V.G. MENON
Theoretical Physics Division, Bhabha Atomic Research Center, Mumbal, India
(RECEIVED 15 July 2005; ACCEPTED 6 November 2005)

**Abstract**

The existing "quotidian equation state" model, based on Thomas-Fermi theory, is modified so as to improve the low density region of phase diagram of metals. A scheme for estimating the critical parameters of liquid-vapor phase transition is proposed. The new model reproduces experimental critical isotherms to a good degree of accuracy. Furthermore, the proposed model is validated with thermodynamic data in the liquid-vapor co-existence region, including results on isobaric expansion as well as released isentropes.

**Keywords:** Critical constants; Isobaric expansion; QEOS; Release isentropes

## 1. INTRODUCTION

The first principle theoretical approaches, like quantum mechanical self-consistent fields, Monte Carlo, and molecular dynamics methods have led to significant progress in constructing the equation of state (EOS) of solid, liquid, and plasma states of matter (Elieser *et al.*, 1986; Bushmann & Fortov, 1983; Ross, 1985). However, all these theories are applicable only in limited ranges. No single theory is able to provide an accurate theoretical estimate of the thermodynamic properties of matter in the entire phase plane. Nevertheless, there are attempts in constructing EOS models that can generate reasonably accurate numerical tables over a wide range of temperature, density, and material composition. Such tabulations are prerequisites for simulations of various high-energy-density dynamic processes. Several laboratories around the world have developed the so called "global EOS models" for this purpose (Abdallah, 1984; Bushmann *et al.*, 1993; Kerley, 1991; More *et al.*, 1988). The quotidian equation of state (QEOS), introduced by More *et al.* (1988), is such a general-purpose model. It is used in hydrodynamic simulations of high pressure phenomena covering wide ranges of density and temperature.

The experimental data, particularly at high temperatures and pressures, plays an important role since they serve as reference points for theories, as well as semi-empirical models. For most metals, barring a few in the alkali group, the liquid region (upto critical temperature) is unattainable for experimentation because of large cohesive energy, and high temperatures and pressures involved. The traditional methods of creating high energy density (HED) matter for experimental investigations involve shock compression of matter. Among the available experimental techniques, shock wave method allows one to study a broad range of phase diagram, from compressed hot dense solid to strongly coupled plasma and two-phase regions (Elieser *et al.*, 1986; Bushmann & Fortov, 1983).

There are recent reports of using intense heavy ion beams along with powerful lasers for experimental study of high-energy-density states of matter (Hoffmann *et al.*, 2002, 2005; Tahir *et al.*, 2005*b*). Further, heavy ion beam driven experiments allow one to access broad unexplored regions of the phase diagram of many materials, particularly in the states of hot liquid region. The detailed investigations of strongly coupled plasmas, warm dense matter, and metallic hydrogen have already been made (Tahir *et al.*, 2005*a*; Temporal *et al.*, 2005).

In this paper, we present a modified QEOS model for constructing wide range tables covering the liquid-vapor co-existence region. A new scheme for estimating the critical constants of liquid metals is proposed. This scheme incorporates improvements in the models for thermal excitation of the electrons and ions. Our scheme is applied to validate the near-critical experimental isotherms for Mercury. For further validation of our model, we make comparisons with experimental data obtained by isobaric expansion and isen-

Address correspondence and reprint requests to: Aditi Ray, Theoretical Physics Division, Bhabha Atomic Research Center, Mumbal, India. E-mail: aray@barc.gov.in

tropic shock unloading. To the best of our knowledge, such evaluations have not been published using QEOS model.

## 2. BRIEF REVIEW OF EARLIER WORK

Starting with Van der Waal's theory (Novikov, 1965) of inpenetrable hard spheres (HS), with a weak long ranged attractive tail, various models have been used up to now to estimate the critical constants of liquid metals. Though the liquid-vapor co-existence curves for metals are nearly quadratic like that of the Van der Waals gas, the theoretical critical compressibility ratio (0.375) differs from experimental values found between 0.2–0.4. As a first step toward improving the Van der Waal's model, Young and Alder (1971) replaced its repulsive component of pressure by a more accurate formula for HS pressure (Carnahan & Starling, 1969). The HS pressure is derived by using the Percus–Yevic theory of dense fluids. The improved model provides critical temperature of alkali metals in agreement with other experiments, but is unable to predict accurate values for the critical volume and pressure.

It was realized that the impenetrable HS theory can not be used for liquid metals, which are known to be compressible. Moreover, the large number of free electrons present in a metal, and the configuration of ions have to be taken into account in the EOS. Young (1977) then replaced the HS model by the so called soft sphere (SS) model introduced by Hoover *et al.* (1975). This model is based on computer calculations for the "effective" free energy of particles in the fluid. The modified SS pressure and energy, in standard notation is given by Young (1977):

$$p = \frac{RT}{V}\left[1 + \frac{1}{3} nC_n \rho^{n/3}\left(\frac{\epsilon}{kT}\right) + \frac{1}{18} Qn(n+4)\rho^{n/9}\left(\frac{\epsilon}{kT}\right)^{1/3} - m\rho^m\left(\frac{\epsilon}{kT}\right)\right] \quad (1)$$

and

$$E = RT\left[\frac{3}{2} + C_n \rho^{n/3}\left(\frac{\epsilon}{kT}\right) + \frac{1}{6} Q(n+4)\rho^{n/9}\left(\frac{\epsilon}{kT}\right)^{1/3} - \rho^m\left(\frac{\epsilon}{kT}\right)\right] + E_{coh}. \quad (2)$$

In the above, $C_n \rho^{n/3}$ represents the static lattice energy term with $C_n$ as the face-centered-cubic (FCC) Medulung constant, and $\rho = N\sigma^3/\sqrt{2}V$. The first term of Eq. (1) refers to the thermal pressure of the ions in the ideal gas approximation. Pressure generated due to thermal excitation of electrons is described by the third term. The second and fourth terms jointly describe the "cold pressure," with $\rho^{n/3}$ and $\rho^m$ dependence arising from repulsion and attraction between neighboring ions. Eq. (2) for energy also has similar interpretation. By adjusting five parameters ($\epsilon$, $\sigma$, $n$, $m$, and $Q$), Young (1977) then obtained the total energy and pressure of a liquid metal at any density and temperature. The critical constants of this model show significant improvements over the HS model. However, there are still discrepancies between SS estimates and the experimental values (Young, 1977). The reason for this discrepancy has not been explained, one possible reason could be that the thermal pressure due to the large number of free electrons needs some further refinements. Also, at this temperature the ions do not really behave like an ideal gas.

## 3. GLOBAL EOS MODEL

In order to construct a more general and thermodynamically complete multi-phase wide range EOS model, like QEOS, one defines the thermodynamic free energy as:

$$F(\rho,T) = F_{cold}(\rho) + F_i(\rho,T) + F_e(\rho,T), \quad (3)$$

which consists of elastic contribution at zero temperature ($F_{cold}$), and the thermal contributions by ions ($F_i$) and electrons ($F_e$). The global QEOS uses this additivity property of free energy. The electronic contributions in this model has been adopted from Thomas–Fermi (TF) statistical model of Feynman *et al.* (1949). However, for density ($\rho$) greater than solid density ($\rho_s$), TF contribution to $F_{cold}$ is supplemented by a semi-empirical bonding correction, originally proposed by Barnes (1967). The ion EOS of this global model combines Debye, Gruneisen, and liquid scaling laws based on the work of Cowan (More *et al.*, 1988). For density lower than solid density, $F_{cold}$ is taken as the zero temperature TF energy. As discussed by More *et al.* (1988), this model leads to over-estimation of the critical pressure and temperature. Also, for some of the materials, the QEOS estimates for the cohesive energy are negative, leading to disappearance of the liquid-vapor region itself, which is totally unphysical.

The problem of over estimation of critical temperature and pressure in the original QEOS model has been addressed by Young and Corey (1995). They replaced the TF cold curve for low density region, $\rho < \rho_s$, with Lennard–Jones type of soft sphere function. According to this model, the cold energy for $\rho < \rho_s$ is given by:

$$E_{cold}(\rho) = A_c \rho^n - B_c \rho^m + E_{coh}, \quad (4)$$

where $E_{coh}$ is the experimental cohesive energy. The coefficients $A_c$ and $B_c$ are estimated by setting the energy and pressure values at standard condition. The exponents $m$ and $n$ are adjustable parameters. The results of this model for critical temperature and pressure are not in very good agreement with experimentally known values for metals (Young & Corey, 1995). Morever, difficulties arise when one tries to reproduce the critical isotherm for any metal using the

https://doi.org/10.1017/S0263034606060381 Published online by Cambridge University Press

reported values of $m$ and $n$. It is also reported (Young & Corey, 1995) that this model is not able to verify the liquid-gas co-existence region with the experimental isobaric expansion data (Gathers, 1986) for most of the metals.

One of the main aims of the present work is to show that, for obtaining the correct set of critical constants and liquid-gas phase boundary, it is necessary to model the electron and the ion thermal pressure more appropriately.

## 4. PROPOSED SCHEME

Following the QEOS approach, we have constructed a global theoretical EOS model assuming the additivity of electron, and ion free energies for all temperature and density. Accordingly, we express the total energy for $\rho < \rho_s$ as:

$$E_{tot}(\rho,T) = E_{th}(\rho,T) + E_{cold}(\rho), \tag{5}$$

where

$$E_{th}(\rho,T) = E_e(\rho,T) + E_i(\rho,T), \tag{6}$$

is the thermal energy of the electrons and ions, and $E_{cold}$ is the cold energy. The total pressure defined as:

$$p_{tot}(\rho,T) = \rho^2 \left( \frac{\partial^2 E_{tot}}{\partial \rho^2} \right)_T, \tag{7}$$

assumes the form:

$$p_{tot}(\rho,T) = p_{th}(\rho,T) + p_{cold}(\rho), \tag{8}$$

where $p_{cold}$ refers to the cold pressure. $p_{th}$ is the thermal pressure arising due to electrons and ions, that is,

$$p_{th}(\rho,T) = p_e(\rho,T) + p_i(\rho,T). \tag{9}$$

In this paper, we are proposing a scheme for determining the EOS of metals in the liquid-vapor region, that compares the experimental results. The new scheme is based on the use of more experimental data for physical and thermodynamic parameters, like melting temperature, electron specific heat, etc. We also propose a simple approach for finding the parameters of SS function defining the cold part. In the following subsections, we discuss the improvements in electron and ion contribution to EOS, and cold part separately.

### 4.1. Ion EOS

The ion thermal pressure in the QEOS model has been estimated by the structural and phenomenological models of Cowan. We also treat the ion contribution to EOS by Cowan's model, however, with some modifications. Depending on the temperature of interest, Cowan's model treats ions in three distinct phases, namely, the low-temperature solid phase, followed by high temperature solid, and finally fluid phase. The fluid phase is reached when temperature is greater than the melting temperature of the solid. Since we are interested in the liquid-vapor phase transition region, we will consider the fluid region only, that is $T > T_m$. Following More *et al.* (1988), we express the energy and the pressure of the ions in this region as:

$$E_i(\rho,T) = \frac{3}{2} \frac{kT}{AM_p} (1 + w^{1/3}), \tag{10}$$

$$p_i(\rho,T) = \frac{\rho kT}{AM_p} (1 + \gamma_F w^{1/3}), \tag{11}$$

where, $w = T_m(\rho)/T$ and $\gamma_F$ are the fluid phase. Gruneisen (1912) parameter, which depends on density through the relation

$$\gamma_F = \frac{3}{2} \frac{\partial \log(T_m(\rho))}{\partial \log(\rho)}. \tag{12}$$

From Eqs. (10) and (11), it can be easily seen that for very high temperature, $T \gg T_m$, or $w \ll 1$, ion internal energy and pressure reduce to the ideal gas expressions, that is,

$$E_i(\rho,T) = \frac{3}{2} \frac{kT}{AM_p}, \quad p_i(\rho,T) = \frac{\rho kT}{AM_p}. \tag{13}$$

As the temperature at which the liquid-gas phase transition takes place is much higher than the melting temperature of metals, the ideal gas treatment of Young (1977) in the SS model was not in serious error. But this is not true in general.

We modify the ion model with the observation by More *et al.* (1988) that there are important differences between Cowan model melting temperatures with the corresponding experimental values for transition metals, even at normal density $\rho_s$. This resulted in over-estimation of the critical pressure in QEOS. To that end, we normalized Cowan's melting temperature at $\rho_s$ with the corresponding experimental value, and express it as:

$$T_m^{cor}(\rho) = T_m^{Cowan}(\rho) \frac{T_m^{Exp}(\rho_s)}{T_m^{Cowan}(\rho_s)}, \tag{14}$$

where $T_m^{cor}$ refers to the corrected melting temperature. It can be easily shown from Eq. (12) that the fluid phase Gruneisen (1912) parameter, remains unaltered with this correction. We find that this correction improves the critical pressure for transition metals significantly.

### 4.2. Electron EOS

In all the global models, including QEOS, the electron contribution has been treated by the TF theory. However, we know that the TF theory gives an accurate representation of

https://doi.org/10.1017/S0263034606060381 Published online by Cambridge University Press

the free electron pressure for temperatures above ~10 eV. The largest inaccuracy in the TF electron pressure occurs near the solid density and $T = 0$. Since the critical temperature for most of the elements are less than 2 eV, the TF theory is not a very good candidate for treating the liquid-gas region. Therefore, electron thermal pressure, in the region $\rho < \rho_s$, needs adjustment with some experimental data .

In our model, we use McCloskey's (1964) semi-empirical formula for estimating the contribution to pressure from thermal excitation of electrons. Therefore, the thermal energy and pressure at any temperature are given by

$$E_e(\eta, T) = \frac{9r^2}{4\beta(\rho)} \log\cosh\left(\frac{2\beta(\rho)T}{3r}\right),$$
$$p_e(\eta, T) = \eta\rho_s \frac{r^2}{\Gamma_e\beta(\rho)} \log\cosh\left(\frac{\Gamma_e\beta(\rho)T}{r}\right). \quad (15)$$

In these equations, $T$ is in eV, $Z$ is the atomic number of the element, $\eta = \rho/\rho_s$ and $\beta(\rho)$ is the coefficient of electronic specific heat. The following fitting formulas are used for other parameters in Eq. (15):

$$r = \frac{0.85X^{0.59}}{1 + 0.85X^{0.59}} ZR, \quad X = \frac{1}{Z^{4/3}} T, \quad \Gamma_e = 0.5 - 0.6. \quad (16)$$

Note that for very high temperature, the energy and the pressure relations given in (15) reduce to that of ideal electron gas, that is,

$$E_e(\eta, T) = \frac{3}{2} RT, \qquad p_e(\eta, T) = \rho RT. \quad (17)$$

On the other hand, for very low temperature, the electron EOS given in (15) reduces to that of a degenerate electron gas

$$E_e(\eta, T) = \frac{1}{2}\beta(\rho)T^2, \qquad p_e(\eta, T) = \frac{1}{2}\rho\Gamma_e\beta(\rho)T^2. \quad (18)$$

Thus, McCloskey's (1964) formula interpolates the electron EOS at any temperature appropriately. The coefficient of electronic specific heat $\beta(\rho)$ depends on the density by the relation

$$\beta(\rho) = \beta_0\left(\frac{\rho_s}{\rho}\right)^{2/3}, \qquad \beta_0 = \frac{4\pi^4}{(3\pi^2)^{2/3}} \frac{k^2 m_e}{h^2} \frac{N_e^{1/3}}{\rho_s^{2/3}}, \quad (19)$$

where, $N_e$ is the number of free electrons per unit mass, and $\beta_0$ is the theoretical estimate for $\beta(\rho_s)$. It is known that the experimental values of $\beta_0$ differ from this estimate for most metals (Kittel, 1971).

On expanding the TF expression for electron energy at very low temperature and keeping the terms up to $T^2$ one obtains Eq. (18), with the theoretical $\beta_0$. Even if one replaces this theoretical estimate of $\beta_0$ with its experimental value, the question whether the temperature is sufficiently low for such expansion remains debatable. Both the facts cause TF theory to estimate the electron pressure incorrectly. In this regard, McCloskey (1964) formula seems to be a better choice, as it finds the energy and pressure for any temperature by using proper fitting constants. We therefore used McCloskey's formula together with the measured value of $\beta_0$. This approach provides the correct electron pressure and energy upto about two to three times the critical temperature. Above this temperature, the TF theory is appropriate.

### 4.3. Cold Curve

Following Al'tshuler *et al*. (1980), we express the cold energy as:

$$E_{cold}(\rho) = A\rho_r^m - B\rho_r^n + E_{coh}, \quad (20)$$

where $E_{coh}$ is the experimental cohesive energy and $\rho_r = \rho/\rho_s$. Hence, the cold pressure is

$$p_{cold}(\rho) = \rho_s[Am\rho_r^{m+1} - Bn\rho_r^{n+1}]. \quad (21)$$

The parameters $A$ and $B$ are obtained by the requirements that the total energy and pressure vanishes at $\rho = \rho_s$ and $T = 0$. Thus we get

$$A = \frac{nE_{coh}}{m-n}, \qquad B = \frac{mE_{coh}}{m-n}. \quad (22)$$

With the help of Eq. (22), we can now rewrite the expression for the cold energy and pressure as:

$$E_{cold}(\rho) = \frac{E_{coh}}{m-n}[n\rho_r^m - m\rho_r^n] + E_{coh} \quad (23)$$

and

$$p_{cold}(\rho) = \rho_s E_{coh} \frac{mn}{m-n}[\rho_r^{m+1} - \rho_r^{n+1}]. \quad (24)$$

Thus, the total pressure of Eq. (8) reduces to

$$p_{tot}(\rho, T) = p_{th}(\rho, T) + \rho_s E_{coh} \frac{mn}{m-n}[\rho_r^{m+1} - \rho_r^{n+1}]. \quad (25)$$

Using the expressions for thermal pressure of ions (Eq. (11)) and electrons (Eq. (15)), we obtain

$$p_{tot}(\rho, T) = \frac{\rho kT}{AM_p}(1 + \gamma_F w^{1/3}) + \eta\rho_s \frac{r^2}{\Gamma_e\beta(\rho)} \log\cosh\left(\frac{\Gamma_e\beta(\rho)T}{r}\right)$$
$$+ \rho_s E_{coh} \frac{mn}{m-n}(\rho_r^{m+1} - \rho_r^{n+1}). \quad (26)$$

https://doi.org/10.1017/S0263034606060381 Published online by Cambridge University Press

In next section, we present our approach for finding the exponents $m$ and $n$.

## 5. FINDING CRITICAL CONSTANTS

Our formulation for total pressure can now be used to determine the critical constants for metals. Instead of adjusting the parameters $m$ and $n$ arbitrarily, we find them explicitly using a set of experimental values for certain thermodynamic variables. First, we match the bulk modulus calculated by using Eq. (26) with it's experimental value, $B_0$, at solid density $\rho_s$, that is,

$$\left(\rho \frac{\partial p_{tot}}{\partial \rho}\right)_{\rho_s} = B_0. \tag{27}$$

Since the thermal contribution to pressure $p_{th}$ is zero at $T = 0$ and $\rho = \rho_s$, Eqs. (26) and (27) give

$$\rho_s nxE_{coh} + \rho_s n^2 E_{coh} = B_0, \tag{28}$$

where we have introduced a new variable $x$ defined as:

$$x = m - n. \tag{29}$$

Eq. (28) is rewritten as:

$$x = \frac{B_0 - \rho_s n^2 E_{coh}}{\rho_s n E_{coh}}. \tag{30}$$

From the definition of cold pressure, it is evident that $m$ and $n$ are both positive and $m > n$. Hence, $x$ is also positive. The positivity of $x$ demands that $n$ is bounded above by:

$$n < \sqrt{\frac{B_0}{\rho_s E_{coh}}} = y_0 \quad \text{(say)}. \tag{31}$$

Next we follow the steps outlined below:

1. Choose the experimental value of $B_0$ at $\rho = \rho_s$.
2. Estimate critical temperature $T_c$ either by the Partington (1949) formula or Jing's modification (1984), wherein it is shown that the critical temperature is related to the sum of melting and boiling temperatures. Now, choose a temperature $T_a$ close to this estimate.
3. Choose a value of $n$ much smaller than $y_0$.
4. Find $x$ and hence, $m$ using Eqs. (30) and (29), and use Eq. (26) to get total pressure at the chosen temperature $T_a$.
5. As we know that the first and second derivatives of total pressure vanish at $T_c$, determine densities $\rho_1$ and $\rho_2$ using the relations:

$$\left(\frac{\partial p_{tot}}{\partial \rho}\right)_{T_a} = 0, \qquad \left(\frac{\partial^2 p_{tot}}{\partial \rho^2}\right)_{T_a} = 0. \tag{32}$$

6. If $\rho_1$ and $\rho_2$ are equal to the required accuracy, then accept this density as the critical density, that is, $\rho_c = \rho_1 = \rho_2$. Thus the chosen temperature is nothing but the critical temperature, $T_c = T_a$. Finally the critical pressure is $p_c = p_{tot}(\rho_c, T_c)$.
7. If $\rho_1$ and $\rho_2$ are not the same, increase the value of $n$ by a small amount and repeat from step 3.
8. If necessary, repeat the procedure from step 2 by increasing $T_a$ until the correct set of exponents ($m$ and $n$) are obtained for which $\rho_1$ and $\rho_2$ are the same.
9. If the above steps are not successful then change the value of $B_0$ and follow the steps 2–8. We find that the value of $B_0$ that staisfies the condition given in step 5 happens for less than its experimental value at $\rho_s$. This is due to the fact that slopes of the pressure-density curve at two sides of the solid density are slightly different. The value of $B_0$ is further tuned so as to match other experimental results described in the next section.

We have applied the above described approach to predict the critical constants for all metals. Table 1 presents the values of the Lennard–Jones exponent $m$ and $n$, and the parameters of critical points for 10 metals obtained by our method, along with other theoretical estimates and experimental results, if available. For most of the metals, our estimates of critical temperature are lower than the hard-sphere model of Young and Alder (1971) and higher than the soft-sphere model (Young, 1977).

For Mercury, our estimate of all the four parameters including the critical compressibility ratio, $Z_c = p_c/R\rho_c T_c$, are very close to experimental values. However, our predicted value of $p_c$ for Lead is higher than other evaluation, leading to larger $Z_c$.

## 6. VALIDATION OF THE PROPOSED MODEL

For validating our model, we first compared the predicted and experimental data for the critical isotherm of Mercury (Young & Alder, 1971). Figure 1 shows the density dependence of pressure (both normalized to their respective critical values) for temperatures $T = 1.01\ T_c$ and $T = 1.13\ T_c$, with solid lines corresponding to our results and points refering to experimental values. The agreement is quite satisfactory.

### 6.1. Isobaric Expansion

The thermodynamic properties of a metallic liquid are studied either by density measurements at normal pressure (Lang, 1995), or by isobaric expansion techniques (Gathers, 1986). In the second technique, the metal is rapidly heated by a powerful pulse of current and then allowed to expand in an

https://doi.org/10.1017/S0263034606060381 Published online by Cambridge University Press

**Table 1.** *Estimations of Lennard–Jones and critical parameters for metals*

| Element | m | n | $T_c$ K | $\rho_c$ (g/cc) | $P_c$ (Kbar) | $Z_c$ | Ref. |
|---|---|---|---|---|---|---|---|
| Na | 5.4823 | 0.5898 | 2448 | 0.20 | 0.48 | 0.27 | a |
| | | | 2573 | 0.21 | 0.28 | 0.15 | v |
| | | | 2429 | 0.16 | 0.30 | 0.21 | c |
| | | | 2573 | 0.22 | 0.55 | 0.27 | e |
| | | | 2573 | 0.20 | 0.35 | 0.2 | Ex |
| Al | 1.9508 | 0.4531 | 5700 | 0.32 | 1.87 | 0.33 | a |
| | 2.0 | 0.5 | 5520 | — | 1.68 | — | d |
| | | | 5726 | 0.42 | 1.82 | 0.24 | c |
| | | | 7151 | 0.69 | 5.45 | 0.36 | b |
| Fe | 1.8988 | 0.6950 | 6900 | 1.77 | 8.82 | 0.48 | a |
| | | | 9600 | 2.03 | 8.25 | 0.28 | v |
| | | | 9340 | 1.71 | 8.03 | 0.34 | e |
| | | | 9340 | 2.03 | 10.15 | 0.36 | b |
| Cu | 2.3857 | 0.6727 | 7800 | 2.31 | 8.94 | 0.38 | a |
| | | | 7830 | 2.13 | 9.07 | 0.41 | f |
| | | | 7625 | 2.32 | 8.3 | 0.36 | b |
| | | | 8400 | 1.76 | 6.08 | 0.32 | r |
| Mo | 3.2131 | 0.4887 | 9500 | 2.82 | 9.64 | 0.41 | a |
| | | | 16140 | 3.18 | 12.63 | 0.28 | v |
| | 2.0 | 0.65 | 10500 | — | 8.8 | — | d |
| | | | 14300 | 3.03 | 5.68 | 0.15 | h |
| | | | 8002 | 1.02 | 9.7 | 0.61 | c |
| | | | 14588 | 2.61 | 11.8 | 0.36 | b |
| Hg | 4.6765 | 0.747 | 1755 | 5.99 | 1.65 | 0.38 | a |
| | 3.4 | 1.05 | 1080 | — | 1.23 | — | d |
| | | | 2074 | 4.27 | 1.78 | 0.53 | c |
| | | | 1563 | 3.97 | 0.92 | 0.35 | b |
| | | | 1570 | 4.77 | 0.91 | 0.29 | r |
| | | | 1753 | 5.73 | 1.52 | 0.367 | Ex |
| Pb | 1.4414 | 1.3008 | 5400 | 2.80 | 4.01 | 0.66 | a |
| | 2.3 | 1.0 | 4660 | — | 2.97 | — | d |
| | | | 5530 | 3.12 | 2.37 | 0.34 | f |
| | | | 5158 | 3.06 | 2.26 | 0.36 | c |
| | | | 5500 | 2.52 | 2.08 | 0.37 | e |
| | | | 4668 | 3.11 | 2.08 | 0.38 | b |
| Ta | 2.6315 | 0.5568 | 9900 | 4.19 | 10.6 | 0.56 | a |
| | 3.0 | 0.5 | 10400 | — | 7.92 | — | d |
| | | | 9284 | 4.23 | 9.99 | 0.55 | c |
| | | | 17329 | 4.27 | 12.2 | 0.36 | b |
| W | 2.6278 | 0.4635 | 12000 | 4.04 | 10.21 | 0.46 | a |
| | | | 21010 | 5.78 | 15.83 | 0.28 | v |
| | | | 13400 | 4.28 | 3.37 | 0.13 | g |
| | | | 14100 | 5.88 | 5.09 | 0.14 | h |
| | | | 18538 | 4.91 | 14.8 | 0.36 | b |
| U | 6.5917 | 0.3989 | 7000 | 8.11 | 7.11 | 0.36 | a |
| | | | 11630 | 5.3 | 6.11 | 0.28 | v |
| | | | 6618 | 4.11 | 4.16 | 0.43 | c |
| | | | 13043 | 4.07 | 8.53 | 0.46 | e |
| | | | 13043 | 5.18 | 8.48 | 0.36 | b |

(a) This work; (b) (Young & Alder, 1971); (c) (Young, 1977); (d) (Young & Corey, 1995); (e) (Hornung, 1975); (f) (Al'tshuler *et al*., 1980); (v) (Fortov & Yakubov, 1999); (h) (Seydel *et al.*, 1979); (g) (Fucke & Seydel, 1980); (r) (Morris, 1964); (Ex) (Dillon *et al.*, 1966); (Young, 1977).

atmosphere of an inert gas maintaining a prescribed constant pressure $P_{IEX}$. The density, enthalpy at melting and the sound velocity are then measured at different temperatures. On extrapolation, these data embraces the critical density $\rho_c$. In order to compare these liquid metal expansion data, we determine the densities $\rho_i$ and the corresponding temperatures $T_i$ for which the total pressure given in (26) is equal to $P_{IEX}$, by an interpolation method.

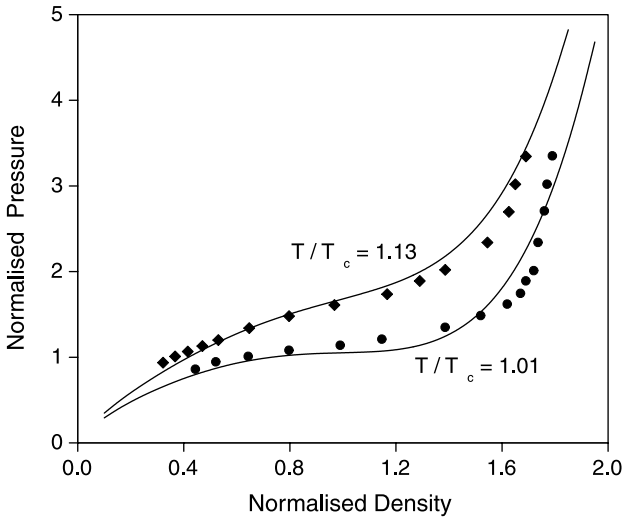


**Fig. 1.** Comparison of experimental isotherm with our model for Mercury.

In Figure 2 we show comparisons for Aluminum, Tantalum, and Lead, with solid lines and points refering to our calculation and measured data, respectively.

Next, we find the total energy for the above values of density and temperature, that is, $E_i = E_{tot}(\rho_i, T_i)$ and then calculate the enthalpy as $H_i = E_{tot}(\rho_i, T_i) + P_{IEX}/\rho_i$. We show the experimental and calculated values of enthalpy for Aluminum, Tantalum, and Lead in Figure 3. It is clear from these figures that the enthalpy data agrees quite well for all the elements. The experimental data used are taken from Gathers (1983*a*, 1983*b*) and Shaner *et al.* (1977).

### 6.2. Release Isentrope

The study of release isentrope of strongly compressed materials provide another way to characterize the liquid-vapor phase region. Release isentrope experiments to cover the complete liquid-vapor region uses porous materials (Al'tshuler *et al.*, 1980), which has not been incorporated in the present model. However, for the normal metals, the release isentrope usually corresponds to the solid and partially melted regions, which has been tested by our model.

The experimental data on release isentropes of shocked solids, in the form of unloading pressure versus free-surface velocity, give indirect information about the phases of the material it passes through while shock unloading. A released isentrope corresponds to specific values of initial shock pressure $P = P_{ri}$ and particle velocity $U_p = U_{ri}$. As the shock unloads at a free-surface, pressure decreases to zero and free-surface velocity increases to two times $U_{ri}$. This increase is due to the isentropic conversion of internal energy to kinetic energy.

https://doi.org/10.1017/S0263034606060381 Published online by Cambridge University Press

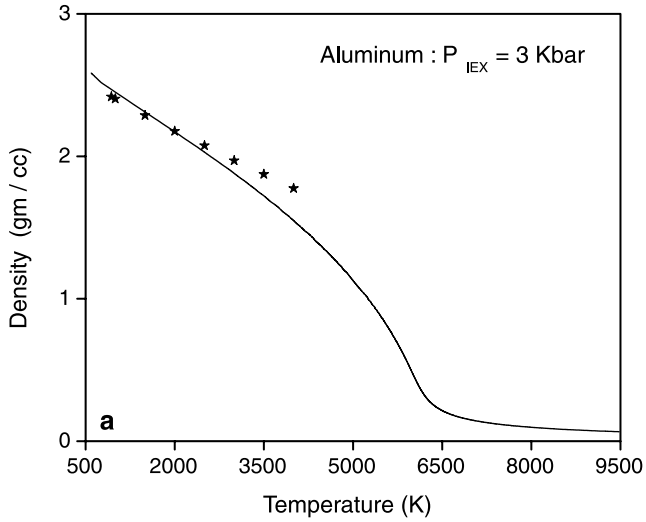


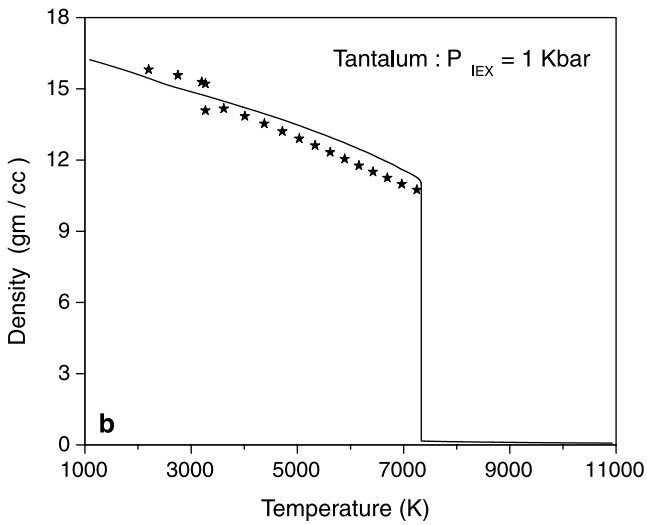


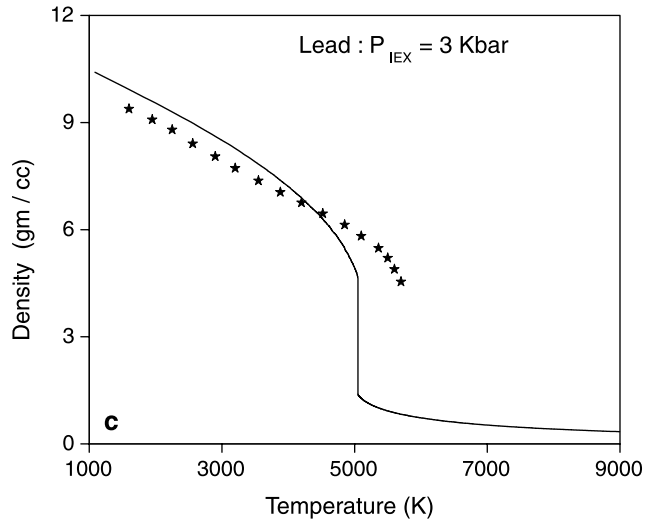


**Fig. 2.** The comparison of isobaric expansion data. Density versus temperature for (**a**) Aluminum, (**b**) Tantalum, and (**c**) Lead. The experimental values are shown by points whereas lines refer to our model result.

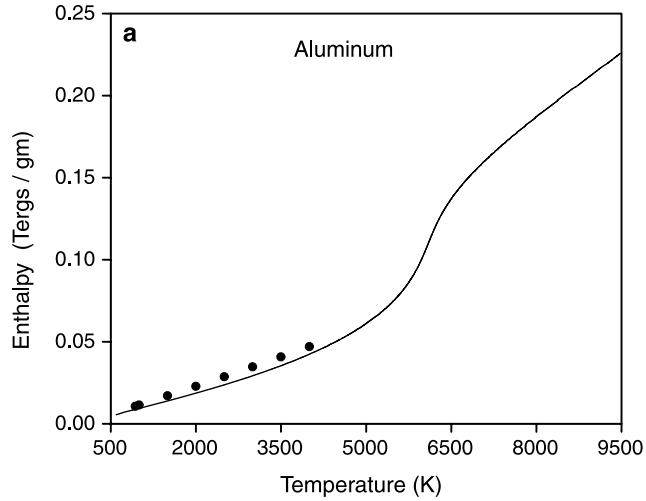


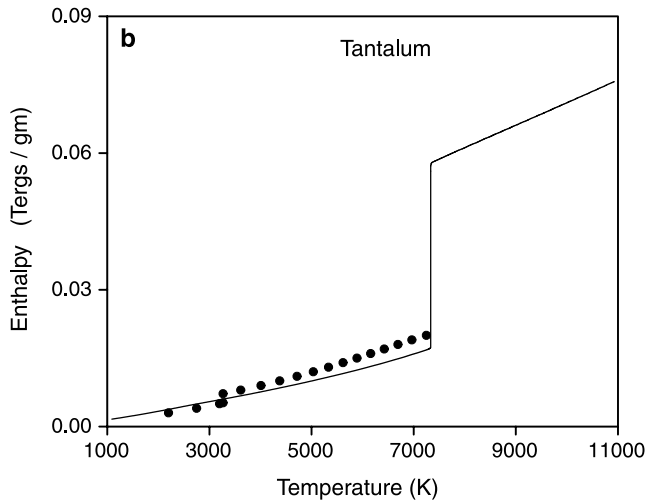


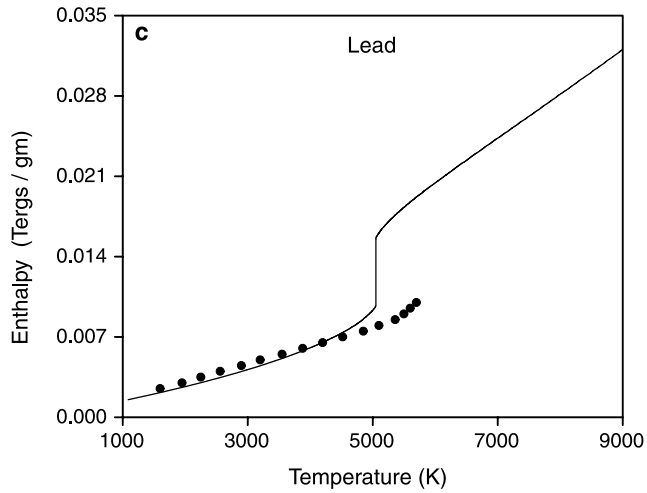


**Fig. 3.** Comparison of isobaric expansion data. Enthalpy versus temperature for (**a**) Aluminum, (**b**) Tantalum, and (**c**) Lead. The experimental values are shown by points whereas lines refer to our model result.

https://doi.org/10.1017/S0263034606060381 Published online by Cambridge University Press

Starting with given $P = P_{ri}$ and $U_p = U_{ri}$, we used the following Hugoniot relations

$$U_p = U_s(1 - \rho_s/\rho), \qquad P = \rho_s U_s U_p, \tag{33}$$

to obtain the initial shock speed $U_s$, and the compressed solid density, $\rho_{ri}$ as:

$$\rho_{ri} = \frac{\rho_s P_{ri}}{P_{ri} - \rho_s U_{ri}^2}. \tag{34}$$

From our model, we also find the entropy $S_{ri}$ of the compressed state corresponding to $\rho_{ri}$ and $P_{ri}$. This entropy identifies the unloading isentrope.

We then use the Riemann invariant condition to estimate the isentropic flow, that is,

$$U_p + \int \frac{dp}{\rho C_s} = \text{constant}. \tag{35}$$

where $C_s = \sqrt{dp/d\rho}$ refers to the isentropic sound speed. The free-surface velocity, $U_2$ corresponding to any lower pressure $P_2$ is then obtained as:

$$U_2 = U_{ri} + \int_{P_2}^{P_{ri}} \frac{dp}{\rho C_s}, \tag{36}$$

which can also be expressed as:

$$U_2 = U_{ri} + \int_{\rho_2}^{\rho_{ri}} C_s \frac{d\rho}{\rho} \tag{37}$$

For $\rho_2$ very close to $\rho_{ri}$, this can be approximated as:

$$U_2 \approx U_{ri} + C_s \log \frac{\rho_{ri}}{\rho_2}. \tag{38}$$

where we have approximated $C_s$ inside the integral with $C_s(\rho_{ri})$.

Using an interpolation method, we first generate the isentrope corresponding to $S_{ri}$. Then eq. (38) is applied successively, by replacing $U_{ri}$ and $\rho_{ri}$ with $U_2$ and $\rho_2$ respectively. Thus we generate the free-surface velocity vs pressure curve along the isentrope. In Figure 4 we show the experimental (points) and calculated (lines) results for Copper and Molybdenum. The experimental results are taken from (Zhernokletov *et al.*, 1984; Zhernokletov *et al.*, 1995). The good agreement observed in these figure validates our model further.

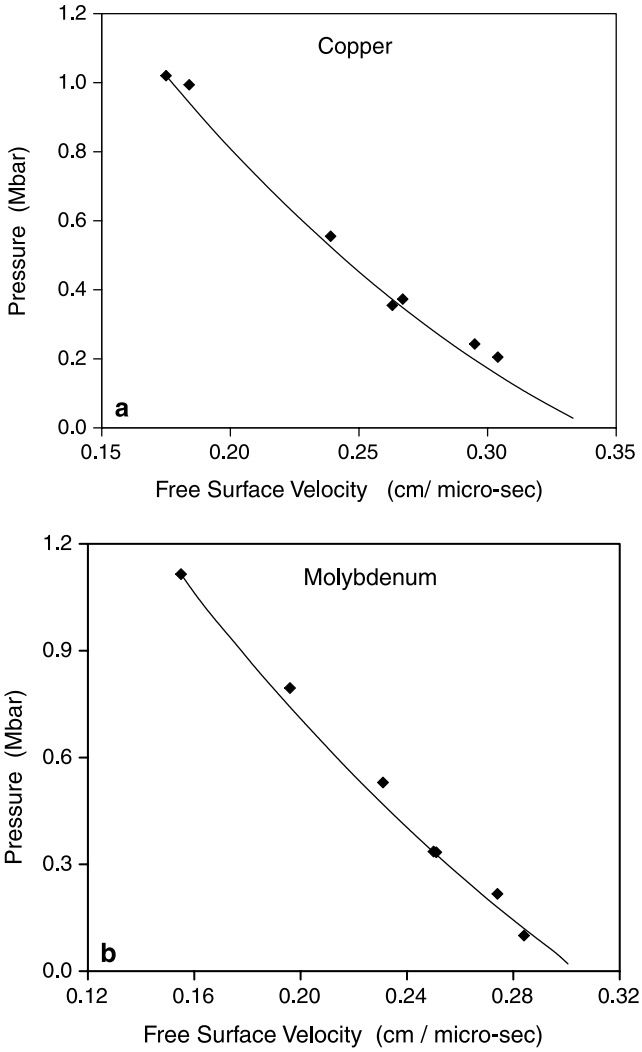


**Fig. 4.** Comparison of isentropic expansion data. The pressure versus free-surface velocity for (**a**) Copper and (**b**) Molybdenum. The lines correspond to our model and points refer to experimental data.

## 7. SUMMARY AND CONCLUSIONS

In this paper, we have introduced certain improvements to the QEOS model so as to generate wide range EOS database in the liquid-vapor phase region.

First of all, we have identified that the contributions to thermal pressure by ions and electrons need certain improvements. To that end, we have introduced a scaling of melting temperature in the Cowan's model, thereby adjusting it to the experimental value at solid density. Thermal contributions to ion pressure and energy are, therefore, accounted more accurately. In leiu of TF theory, we have introduced McCloskey's semi-empirical formula for the thermal part of electron energy and pressure. This recipe was needed to incorporate the experimental value of low temperature electronic specific heat into the model and to obtain accurate electron EOS for temperatures less than about 3 eV. While the Lennard–Jones soft sphere model for cold pressure is retained, we have evolved a simple scheme to determine its parameters, particularly the nonlinear exponents.

We have applied the modified QEOS model to analyze a few sets of experimental data pertaining to the liquid-vapor

https://doi.org/10.1017/S0263034606060381 Published online by Cambridge University Press

region. These include two isotherms of Mercury, isobaric expansion data for Aluminum, Tantalum and Lead and shock unloading data for Copper and Molybdenum. Comparisons of the model with experimental data show good agreement. Critical point parameters of these materials are also predicted more accurately. Thus, our modifications have resulted in an improved theoretical EOS model which can now be used throughout the phase plane.

## REFERENCES


Abdallah, J., Jr. (1984). Users manual for GRIZZLY. Report No. LA-10244-M. Los Alamos, NM: Los Alamos National Laboratory.

Al'tshuler, L.V., Bushmann, A.V., Zhernokletov, M.V., Zubarev, V.N., Leont'ev, A.A. & Fortov, V.E. (1980). Unloading isentropes of the equation of state of metals at high energy densities. *Sov. Phys. JETP* **51**, 373.

Barnes, J.F. (1967). Statistical atom theory and the equation state of solids. *Phys. Rev.* **153**, 269.

Bushmann, A.V. & Fortov, V.E. (1983). Equation of state models for matter. *Sov. Phys. Usp.* **26**, 465.

Bushmann, A.V., Lomonosov, I.V. & Fortov, V.E. (1993). *Sov. Tech. Rev. B. Therm. Rev.* **5**, 1.

Carnahan, N.F. & Starling, K.E. (1969). Equation of state for nonattracting rigid spheres. *J. Chem. Phys.* **51**, 635.

Dillon, I.G., Nelson, P.A. & Swanson, B.S. (1966). Measurement of densities and estimation of critical properties of the alkali metals. *J. Chem. Phys.* **44**, 4229.

Elieser, S., Ghatak, A.K. & Hora, H. (1986). *An Introduction to Equations of state: Theory and Applications*. Cambridge, UK: Cambridge University Press.

Feynman, R.P., Metropolis, N. & Teller, E. (1949). Equation of state of elements based on the generalized Fermi-Thomas theory. *Phys. Rev.* **75**, 1561.

Fortov, V.E. & Yakubov, L.T. (1999). *Physics of Non-Ideal Plasmas*. London, UK: World Scientific.

Fucke, U. & Seydel, W. (1980). Improved experimental determination of critical-point data for tungsten. *High Temp. High Pressures* **12**, 419.

Gathers, G.R. (1983*a*). Thermophysical properties of liquid copper and aluminum. *Int. J. Thermophys.* **4**, 209.

Gathers, G.R. (1983*b*). Correction of specific heat in isobaric expansion data. *Int. J. Thermophys.* **4**, 149.

Gathers, G.R. (1986). Dynamic methods for investigating thermophysical properties of matter at very high temperature and pressures. *Rep. Prog. Phys.* **49**, 341.

Gruneisen, E. (1912). Theorie des festen zustandes einatomiger element. *Ann Phys* **12**, 257.

Hoffmann, D.H.H., Blazevic, A., Ni, P., Rosmej, O., Roth, M., Tahir, N.A., Tauschwitz, A., Udrea, S., Varentsov, D., Weyrich, K. & Maron, Y. (2005). Present and future perspectives for high energy density physics with intense heavy ion and laser beams. *Laser Part. Beams* **23**, 47.

Hoffmann, D.H.H., Fortov, V.E., Lomonosov, I.V., Mintsev, V., Tahir, N.A., Varentsov, D. & Wieser, J. (2002). Unique capabilities of an intense heavy ion beam as a tool for equation-of-state studies. *Phys. Plasmas* **9**, 3651.

Hoover, W.G., Stell, G., Goldmark, E. & Degani, G.D. (1975). Generalized van der Waals equation of state. *J. Chem. Phys.* **63**, 5434.

Hornung, K. (1975). Liquid metal coexistence properties from corresponding states and third law. *J. Appl. Phys.* **46**, 2548.

Jing, D.Yi., Tiu-Tung, Y. & Li-Rong, C. (1984). A new relationship for the melting point, the boiling point and the critical point of metallic elements. *J. Phys. F: Metal. Phys.* **14**, L141.

Kerley, G.I. (1991). Users manual for PANDA II: A computer code for calculating equations of state. Report No. SAND88-2291. Albuquerque, NM: Sandia National Laboratories.

Kittel, C. (1971). *Introduction to Solid State Physics*. New Delhi: Wiley.

Lang, G. (1995). *CRC Handbook of Chemistry and Physics* (Lide, D.D., Ed.), Vol. 4, p. 126. Boca Raton, FL: CRC Press.

McCloskey, D.J. (1964). An analytic formulation of equations of state. Report No. RM-3905-PR. Rand Corporation.

More, R.M., Warren, K.H., Young, D.A. & Zimmerman, G.B. (1988). A new quotidian equation state (QEOS) for hot dense matter. *Phys. Fluids* **31**, 3059.

Morris, E. (1964). An application of the theory of corresponding states to the prediction of the critical constants of metal. Report No. 067/64. London, UK: AWRE.

Novikov, I.I. (1965). Remarks on I.I. Novikov's calculation of the critical temperature of the alkali metals. *J. Inorg. Nucl. Chem.* **27**, 1171.

Partington, J.R. (1949). *An Advanced Treatise on Physical Chemistry*. London, UK: Longmans.

Ross, M. (1985). Matter under extreme condition of temperature and pressure. *Rep. Progr. Phys.* **48**, 1.

Seydel, U., Bauhof, H., Fucke, W. & Wadle, H. (1979). Thermophysical data for various transition metals at high temperatures obtained by a submicrosecond-pulse-heating method. *High Temp. High Pressures* **11**, 635.

Shaner, J.W., Gathers, G.R. & Hodgson, W.M. (1977). *Proc. 7th Symp on Thermophysical Properties*, p. 896. New York: ASME.

Tahir, N.A., Goddard, B., Kain, V., Schmidt, R., Shutov, A., Lomonosov, I.V., Piriz, A.R., Temporal, M., Hoffmann, D.H.H. & Fortov, V.E. (2005*a*). Impact of 7-TeV/c large hadron collider proton beam on a copper target. *J. Appl. Phys.* **97**, 08332.

Tahir, N.A., Kain, V., Schmidt, R., Shutov, A., Lomonosov, I.V., Gryaznov, V., Piriz, A.R., Temporal, M., Hoffmann, D.H.H. & Fortov, V.E. (2005*b*). The CERN large hadron collider as a tool to study high-energy density matter. *Phys. Rev. Lett.* **94**, 135004.

Temporal, M., Cela, J.J.L., Piriz, A.R., Grandjouan, N., Tahir, N.A. & Hoffmann, D.H.H. (2005). Compression of a cylindrical hydrogen sample driven by an intense co-axial heavy ion beam. *Laser Part. Beams* **23**, 137.

Young, D.A. & Alder, B.J. (1971). Critical point of metals from the van der Waals model. *Phys. Rev.* **3**, 364.

Young, D.A. (1977). A soft-sphere model for liquid metals. Report No. UCRL-52352. Berkley, CA: Lawrence Livermore Laboratory.

Young, D.A. & Corey, E.M. (1995). A new global equation of state model for hot dense matter. *J. Appl. Phys.* **78**, 3748.

Zhernokletov, M.V., Zubarev, V.N. & Sutulov, Yu.N. (1984). Adiabats of porous samples and expansion iseotropes of copper. *J. Appl. Mech. Techn. Phys.* **25**, 107–110.

Zhernokletov, M.V., Simakov, G.V., Sutulov, Yu.N. & Trunin, R.F. (1995). Unload isentropes of aluminum, iron, molybdenum, lead and tantalum. *Teplofiz. Vys. Tmp.* **33**, 40.